Politecnico di Bari

Repository Istituzionale dei Prodotti della Ricerca del Politecnico di Bari

# “Darker-than-Black” PbS Quantum Dots: Enhancing Optical Absorption of Colloidal Semiconductor Nanocrystals via Short Conjugated Ligands

This is a post print of the following article

*Original Citation:*
“Darker-than-Black” PbS Quantum Dots: Enhancing Optical Absorption of Colloidal Semiconductor Nanocrystals via Short Conjugated Ligands / Carlo, G., Ivan, I., Eduardo, F., Grisorio, R., Suranna, G.P., Giuseppe, G.. - In: JOURNAL OF THE AMERICAN CHEMICAL SOCIETY. - ISSN 0002-7863. - 137:5(2015), pp. 1875-1886. [10.1021/ja510739q]

*Availability:*
This version is available at http://hdl.handle.net/11589/3152 since: 2021-03-11

*Published version*
DOI:10.1021/ja510739q

Publisher:

*Terms of use:*

(Article begins on next page)

27 November 2026

# ‘Darker-than-Black’ PbS Quantum Dots: Enhancing Optical Absorption of Colloidal Semiconductor Nanocrystals via Short Conjugated Ligands

*Carlo Giansante,*[†,‡] Ivan Infante,[◊] Eduardo Fabiano,[†,‡] Roberto Grisorio,[#] Gian Paolo Suranna,[#] Giuseppe Gigli[†,‡,§]*

*[†] Center for Biomolecular Nanotechnologies @UNILE, Istituto Italiano di Tecnologia, via Barsanti 1, 73010 Arnesano (LE), Italy*

*[‡] NNL-CNR Istituto di Nanoscienze, via per Arnesano, 73100 Lecce, Italy*

*[◊] Kimika Fakultatea, Euskal Herriko Unibersitatea and Donostia International Physics Center (DIPC), 20080, CP1072, San Sebastian, Spain*

*[#] DICATECh - Dipartimento di Ingegneria Civile, Ambientale, del Territorio, Edile e di Chimica, Politecnico di Bari, via Orabona 4, 70125 Bari, Italy*

*[§] Dipartimento di Matematica e Fisica ‘E. De Giorgi’, Università del Salento, via per Arnesano, 73100 Lecce, Italy*

**Abstract.** Colloidal quantum dots (QDs) stand among the most attractive light-harvesting materials to be exploited for solution-processed photovoltaic and photodetection applications. To this aim, replacement of the bulky electrically-insulating ligands at the QD surface coming from the synthetic procedure is mandatory. Here we present a conceptually novel approach to design light-harvesting nanomaterials demonstrating that QD surface modification with suitable short conjugated organic molecules permits to drastically enhance light absorption of QDs, while preserving good long-term colloidal stability. Indeed, rational design of the pending and anchoring moieties which constitute the replacing ligand framework leads to broadband increase of the optical absorbance larger than 300 % for colloidal PbS QDs also at high energies (> 3.1 eV), despite previous reports on size independence of the absorption coefficient. We attribute such a drastic absorbance increase to ground-state ligand/QD electronic coupling, as inferred by density functional theory calculations; moreover, our findings suggest that the optical band gap reduction commonly observed for PbS QD solids treated with thiol-terminating ligands can be prevalently ascribed to 3p orbitals localized on anchoring sulfur atoms which mix with the highest occupied states of the QDs. More broadly, we provide evidence that organic ligands and inorganic cores are inherently electronically coupled materials, thus giving rise to peculiar chemical species which display emerging (optical) properties that cannot be described as the mere sum of those of the ligand and QD components.

**For Table of Contents Only.**



**Introduction.**

Colloidal semiconductor quantum dots (QDs) are particularly attractive as light-harvesting materials for cost-effective optoelectronic applications due to their tunable bandgap, large absorption coefficients, and compatibility with liquid-phase processing.[1] In most cases, such solution processability is guaranteed by organic ligands which are already introduced during QD synthetic procedure to control nucleation and growth and to remove unsaturated valences;[2] however, these pristine ligands are generally electrically-insulating long-chain aliphatic compounds and their post-synthesis replacement with shorter molecules is thus essential for QD integration in efficient optoelectronic devices.[3] Indeed, the impact of ligands at the QD surface on photophysical and electronic properties has been widely experimentally[4] and computationally[5] investigated. Here we show that QD surface modification with short conjugated ligands can be exploited to enhance solar-light absorption of colloidal QDs across the entire UV-Vis-NIR spectral range, while preserving good long-term colloidal stability. We demonstrate the possibility to tune such an optical absorption increase above 300 %, also at high energies (> 3.1 eV), for which it has been previously found that (molar) absorption coefficient is not affected by quantum confinement but scales with QD volume,[6] by tailoring the pending and anchoring moieties which constitute the replacing ligand framework.

Organic ligands at the nanocrystal surface generally comprise an anchoring group, which is commonly a Lewis base that coordinates the metal sites at the QD surface removing unsaturated valences, and a pending moiety, which mediates QD interactions with the surroundings and ensures QD colloidal stability (see Scheme 1). Colloidal stability has a prominent role in the evaluation of the surface modification effects on QD photophysical properties permitting the study of isolated QDs free-standing in solution-phase. This has been however a strong limitation in the case of lead-chalcogenide QDs due to their propensity to undergo oxidation,[7] coalescence,[8] and aggregation upon the addition of small molecules as replacing ligands. As a consequence, pristine ligand replacement was prevalently carried out in solid-phase,[9,10,11,12] which prevents complete access of the replacing ligands to the QD surface and limits the investigation of the ligand/QD interface that may be hindered by inter-QD interactions. In order to overcome the limitations of the solid-phase ligand exchange, we have recently proposed a PbS QD surface modification strategy in solution-phase which permits complete replacement of pristine oleate ligands with short benzenethiolate ligands, while preserving good long-term colloidal stability in chlorinated solvents that are commonly used for the solution-based deposition of QDs into smooth dense-packed thin-films;[13,14] moreover, the

good solubility of both ligands and QDs permits to precisely control their concentrations in a closed system, which may instead be hampered by filtering[15] or phase-transfer[16] of QD solutions. Here we further exploit such a solution-phase surface modification approach to describe the replacing ligand effects on the optical absorption properties of colloidal QDs. We have thus employed the p-methylbenzenethiolate ligand (henceforth referred to as $ArS^-$, which has been prepared deprotonating the thiol group in presence of triethylamine, $Et_3N$)[17,18] as a framework which allows systematic modification of the replacing ligand subunits, namely the pending and the anchoring groups (as schematically shown in Scheme 1a). Indeed, we investigated the role of the pending moiety by exploiting thiolate-terminated ligands while introducing in para position of the benzene ring an electron-withdrawing substituent (such as the trifluoromethyl group in $A–ArS^-/Et_3NH^+$ ionic couple) or an electron-donating substituent (as the amino group in $D–ArS^-/Et_3NH^+$ ionic couple) and comparing the effect of the conjugated backbone with that of a saturated analog (AlSH, which is a weaker acid than $Et_3NH^+$, thus deprotonation of aliphatic thiols with $Et_3N$ is prevented).[17,18] We have also introduced different anchoring groups on the p-methylbenzene moiety which differ in their chemical nature (S-, O-, and N-terminated binding groups) and bonding mode (mono- and bi-dentate coordination geometries) namely, dithioate ($ArCS_2^-$, synthesized as $Et_3NH^+$ ionic couple), carboxylate ($ArCO_2^-$, prepared as $Et_3NH^+$ ionic couple), and amine ($ArNH_2$), in order to elucidate the role exerted by the binding moiety on the optical absorption properties of colloidal QDs. The ligand library used in this work is shown in Scheme 1b.

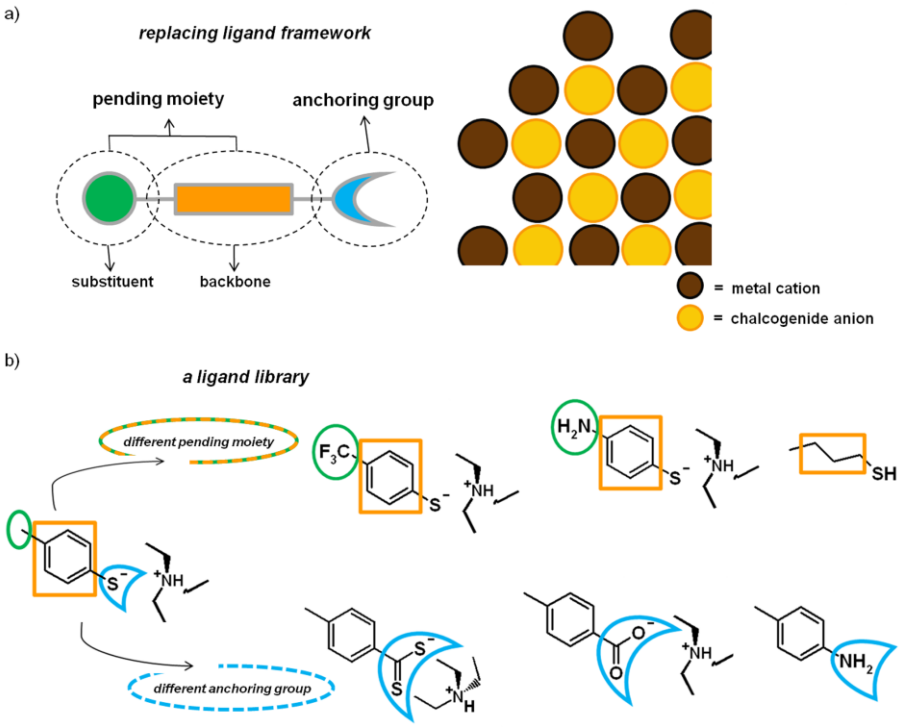


**Scheme 1.** a) Scheme of the replacing ligand framework comprising an anchoring group and a pending moiety, the latter constituted by a backbone which can be further functionalized with chosen substituents. Such ligands are added to solutions of as-synthesized colloidal QDs. b) The library of here employed replacing ligands which bear conjugated or saturated backbone (orange rectangles) further functionalized with electron-donating or withdrawing substituents (green ovals) and differ in the nature and bonding mode of the anchoring group (highlighted in blue). Note that weak acidic character of AlSH prevents its deprotonation with triethylamine ($Et_3N$).

Here we exploit such rational design of the pending and anchoring moieties which constitute the replacing ligand framework to describe and explain the ligand effect on the optical absorption properties of colloidal QDs. The broadband enhancement of optical absorption of colloidal PbS QDs induced by conjugated thiolate-terminated ligands can be tuned above 300 % and is maximized for small QDs in virtue of their large surface-to-volume ratio. These findings disclose the possibility of increasing the absorption coefficient of colloidal QDs also at energies far from the band gap (> 3.1 eV), despite previous reports on size independence of the absorption coefficient.[6] We present density functional theory calculations describing the investigated ligand/QD systems and their ground-state electronic coupling which is at the basis of the observed enhancement of optical absorption, otherwise indescribable as the mere sum of the properties of ligand and QD components. We thus provide a novel path in the design of light-harvesting nanomaterials to be applied in solution-processed photovoltaic and photodetection applications.

**Experimental Section.**

*Materials.* All chemicals were of the highest purity available unless otherwise noted and were used as received. Lead oxide (99.999%), Cadmium oxide (99.5%), oleic acid (technical grade 90%), 1-octadecene (technical grade 90%), bis(trimethylsylil)sulfide (synthesis grade), p-methylbenzenethiol ($ArS^{-}{\cdot}H^{+}$, 98%), p-aminothiophenol (D-$ArS^{-}{\cdot}H^{+}$, 97%), p-(trifluoromethyl)thiophenol (A-$ArS^{-}{\cdot}H^{+}$, 97%), p-toluic acid ($ArCO_2^{-}{\cdot}H^{+}$, 98%), p-toluidin ($ArNH_2$, 99%), 1-butanethiol (AlSH, 99%), were purchased from Sigma-Aldrich. Tri-n-octylphosphine oxide (99%), tri-n-octylphosphine (97%), Sulfur (99%), and Selenium (99,99%) were purchased from Strem Chemicals. Octadecylphosphonic acid (99%) and hexylphosphonic acid (99%) were purchased from Polycarbon Industries. Triethylamine ($Et_3N$, ≥ 99.5%) was purchased from Fluka. All solvents were anhydrous and were used as received. Acetone (99.8%) was purchased from Merck. Acetonitrile (99.8%), chloroform (99.8%), dichloromethane (99.8%), o-dichlorobenzene (99%), hexane (95%), methanol (99.8%), tetrachloroethylene (99%), and toluene (99.8%) were purchased from Sigma-Aldrich.

*QD synthesis.* All QDs were synthesized in a three-neck flask connected to a standard Schlenk line setup under oxygen- and water-free conditions. Details on the synthetic procedures are given in the Supporting Information.

*Synthesis of $ArCS_2^{-}/Et_3NH^{+}$.* A 500 mL round-bottomed flask was filled with magnesium turnings (6.07 g, 0.500 mol) and THF (5 mL) under a nitrogen atmosphere. A solution of 4-bromo-toluene (8.55 g, 0.025 mol) in THF (250 mL) was dropped into the flask with a rate of addition adjusted to maintain a gentle reflux of the resulting mixture. Upon addition of the aryl-bromide, the obtained mixture was refluxed for a further 1 h by an external warming. The solution of the Grignard reagent was cooled to room temperature before addition *via* cannula to a flask containing carbon disufide (11.42 g, 0.150 mol) kept at 0 °C. During the addition, the solution became reddish in appearance. The reaction was quenched with addition of diethyl-ether/water (1/1 vol/vol, 100 mL) followed by dropping conc. HCl to the stirred mixture until the aqueous layer was acidic to the litmus paper. The organic layer was separated, washed with water and dried over $Na_2SO_4$. After solvent removal, the obtained crude violet product was dissolved in hexane (100 mL) and triethylamine (10 mL) was added to the mixture. After 10 min, the triethylammonium salt precipitated as a red powder, that was filtered, washed with hexane and diethyl-ether and dried in vacuo (yield 42%). $^{1}$H-NMR (700 MHz, $CDCl_3$): 8.37 (d, J = 8.2 Hz, 2H), 7.04 (d, J = 8.2 Hz, 2H), 3.25 (q, J = 7.0 Hz, 6H), 2.33 (s, 3H), 1.39 (t, J = 7.0 Hz, 9H) ppm. $^{13}$C-NMR (176 MHz, $CDCl_3$): 253.1, 148.6, 140.3, 127.6, 127.0, 46.0, 21.2, 8.6 ppm. Spectra are shown in the Supporting Information.

*UV-Vis-NIR Absorption Spectroscopy.* The optical absorption spectra of colloidal QDs were measured in quartz cuvettes with 1 cm path length or on glass slides and were recorded with a Varian Cary 5000 UV-Vis-NIR spectrophotometer. Spectrophotometric titration experiments were performed by adding μL aliquots of the replacing ligands' solutions to μM dichloromethane solutions of colloidal QDs in a quartz cuvette.

*Fourier Transform Infrared Spectroscopy (FTIR).* FTIR measurements in the 4000-400 $cm^{-1}$ spectral range were carried out on samples deposited on silicon substrates using a Jasco FT/IR 6300 spectrophotometer apparatus operating in transmission mode at a resolution of 4 $cm^{-1}$.

*Nuclear Magnetic Resonance Spectroscopy (NMR)*. NMR spectra of 0.1 ÷ 1 mM $CDCl_3$ or $C_6D_5CD_3$ solutions were recorded on a 700 MHz Bruker Avance instrument at 298 K.

*Inductively Coupled Plasma Atomic Emission Spectroscopy (ICP-AES).* ICP-AES measurements were performed with a Varian 720-ES spectrometer. The samples for the analyses were prepared by digesting dried QD powders in concentrated $HNO_3$.

*Transmission Electron Microscopy (TEM).* TEM images were recorded with a Jeol Jem 1011 microscope operated at an accelerating voltage of 100 kV. Samples for analysis were prepared by dropping a QD solution onto carbon-coated Cu grids and then allowing the solvent to evaporate in vapor controlled environment.

**Results and Discussion.**

***Quantitative solution-phase ligand exchange.*** The addition of $ArS^-/Et_3NH^+$ to dichloromethane solution of oleate-capped PbS QDs[19] (henceforth referred to as PbS/Ol QDs) induces the displacement of pristine oleate ligands from the QD surface, presumably as $Ol^-/Et_3NH^+$ ionic couple, as suggested by FTIR spectra which show the appearance of the stretching vibration of carbonyl moieties of uncoordinated oleate molecules (around 1700 $cm^{-1}$, grey line in Figure 1a). Complete oleate displacement is demonstrated by the disappearance of carboxylate peaks in FTIR spectra and by the presence of the aromatic ring stretching peculiar of $ArS^-$ (at ~ 1500 $cm^{-1}$, red line in Figure 1a) as a result of the purification which involves quantitative precipitation with excess hexane and redispersion in chlorinated solvents. The effective precipitation of ligand exchanged PbS/ArS QDs with hexane also qualitatively accounts for efficient replacement of oleate ligands: indeed, hexane is a good solvent for PbS/Ol QDs, while it is not for PbS/ArS QDs, hence less apolar solvents have to be used in order to dissolve PbS/ArS QDs, such as dichloromethane (or chloroform, dichlorobenzene). Further confirmation of the quantitative oleate displacement is

provided by $^{1}$H-NMR spectrum of PbS/Ol QDs upon addition of $ArS^{-}/Et_3NH^{+}$ which displays resonance of oleate olefinic protons as a sharp multiplet at lower chemical shifts compared to the broad peak at ~ 5.7 ppm peculiar of oleate molecules bound to QDs (compare blue and grey lines in Figure 1b).[20,21] Successive precipitation of PbS QDs with excess hexane and redispersion in $CDCl_3$ leads to the disappearance of olefinic proton resonance in $^{1}$H-NMR spectrum (red line, Figure 1b), again accounting for the quantitative replacement of pristine oleate ligands from the QD surface.

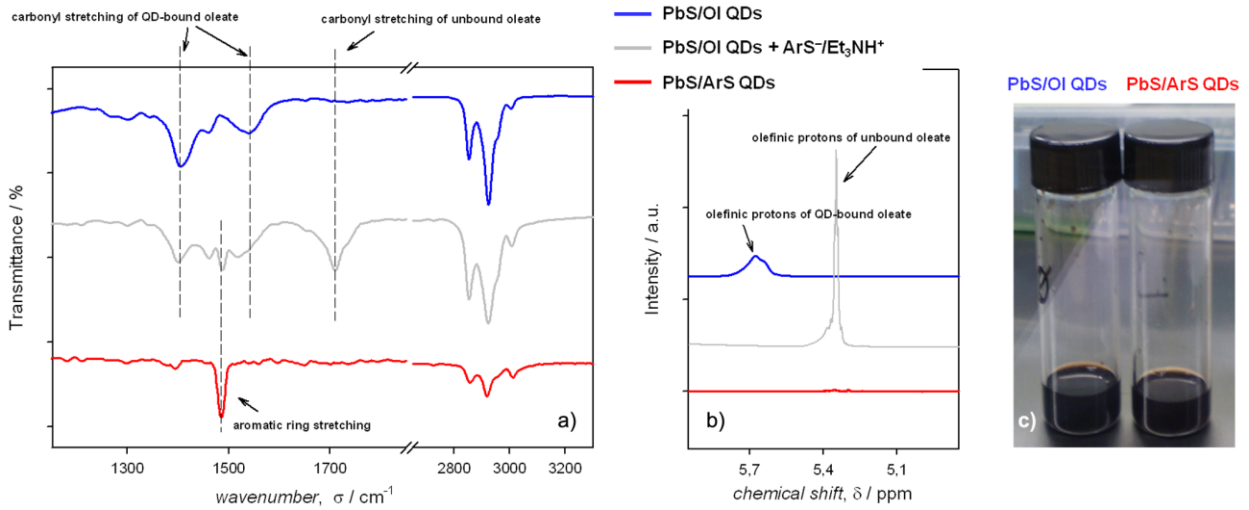


**Figure 1.** a) FTIR spectra of solids of PbS/Ol QDs (blue line), PbS/Ol QDs upon addition of 250 equivalents of $ArS^{-}/Et_3NH^{+}$ (grey line), and purified PbS/ArS QDs (red line). b) $^{1}$H-NMR spectra of 0.1 mM solutions of PbS/Ol QDs (in $C_6D_5CD_3$, blue line), PbS/Ol QDs upon addition of 250 equivalents of $ArS^{-}/Et_3NH^{+}$ (in $CDCl_3$, grey line), and purified PbS/ArS QDs (in $CDCl_3$, red line). Spectra have been vertically offsetted for clarity and spectral features accounting for quantitative oleate-to-arenethiolate exchange have been marked. Breaks have been inserted to highlight such relevant spectral features. Complete FTIR and $^{1}$H-NMR spectra are shown in Supporting Figure S3. c) Daylight picture of three-month old 0.1 mM dichloromethane/dichlorobenzene 1:1 solutions of PbS/Ol QDs (left) and PbS/ArS QDs (right).

***Optical absorption enhancement.*** The addition of $ArS^{-}/Et_3NH^{+}$ to PbS/Ol QDs in dichloromethane solution induces a large increase of the molar absorption coefficient, $\varepsilon$, across the entire UV-Vis-NIR spectral range ($\lambda > 350$ nm) and a bathochromic shift of the first excitonic peak (Figure 2a). The optical absorption spectrum undergoes a sudden modification upon simple mixing of the two components (PbS QDs and $ArS^{-}$ ligands) in a closed system (a quartz cuvette) at room temperature. The modified absorption spectrum is constant with time and does not show any light scattering ascribable to aggregation, as demonstrated by the negligible extinction of the incident light at energies below the first excitonic peak (i. e., $\lambda > 1000$ nm). Furthermore, the observed broadband enhancement of $\varepsilon$

(expressed as $\alpha_{tot}/\alpha_{tot}^0$, where $\alpha_{tot} = \int \varepsilon(\nu)d\nu$ integrated below 3.5 eV and $\alpha_{tot}^0$ the same parameter determined for the as-synthesized PbS/Ol QDs)[22] and the optical band-gap reduction (denoted as $\Delta E_{gap} = E_{gap}^0 - E_{gap}$) reach a plateau at a given $ArS^-$ to QD molar ratio beyond which the absorption spectrum does not appreciably change, suggesting that the PbS QD surface is no longer accessible to extra added $ArS^-$ ligands (see Figure 2b). In order to correlate such a saturation effect to the extent of QD surface modification, we assume in analogy with previous reports that the ligands bind to QD on excess Pb atoms ($Pb_{exc}$).[23,24] Elemental analysis (by ICP-AES) reveals a Pb-to-S molar ratio of 1.8 for as-synthesized PbS/Ol QDs, thus implying that observed optical absorption changes reach a plateau upon the addition of two $ArS^-$ ligands per excess Pb atom (see Figure 2b and Supporting Information for calculation details);[25] moreover, ICP-AES yields a Pb:S molar ratio of 0.66 for ligand-exchanged PbS/ArS QDs confirming the presence of two $ArS^-$ ligands per excess Pb atom in the purified PbS/ArS QD sample.

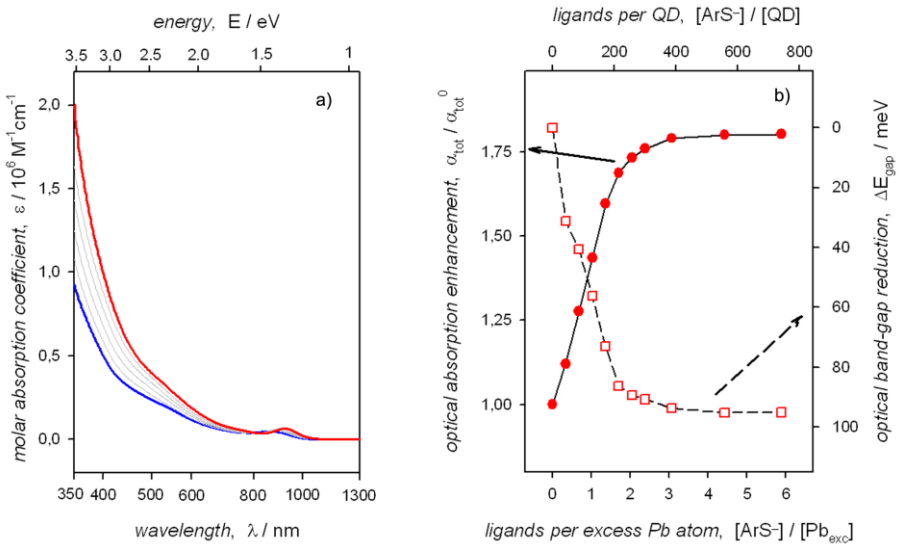


**Figure 2.** a) Absorbance spectra of a dichloromethane solution of colloidal PbS/Ol QDs (blue line), upon addition of $ArS^-/Et_3NH^+$ (grey lines) up to about 750 equivalents (red line). b) Plots of the broadband optical absorption enhancement ($\alpha_{tot}/\alpha_{tot}^0$, full circles) and of optical band-gap reduction ($\Delta E_{gap}$, empty squares) upon addition of $ArS^-/Et_3NH^+$ to PbS/Ol QDs in dichloromethane solution; lines are guide to the eye only.

The observed spectral changes could, in principle, be trivially explained by the addition of absorbing species or by an increase of the QD size. However, the $ArS^-$ ligands show an absorption onset around 300 nm (see absorption spectra of all the replacing ligands employed in this work in Supporting Figure S4) and the observation of a plateau

upon subsequent addition of $ArS^{-}/Et_3NH^{+}$ clearly points to the negligible contribution of the ligand absorption to spectral changes observed below 3.5 eV (or above 350 nm). The growth of the QDs is unlikely to occur in the mild experimental conditions (room temperature) of our solution-phase ligand exchange process; although the diameter changes corresponding to the observed red-shift of the first excitonic peak[6] would correspond to about 0.2 nm (roughly one third of the PbS lattice constant) therefore highly difficult to be experimentally verified, any PbS formation could be optically detected (grey spectrum in Figure S5) upon addition of $ArS^{-}/Et_3NH^{+}$ to Pb(II)-oleate, even upon heating at 110° C, the temperature at which PbS QDs have been synthesized, in accordance with previous reports.[26] The broadband absorbance increase and the red-shift of the first excitonic peak are instead markedly dependent on QD surface-to-volume ratio: indeed, the larger the QD diameter the smaller the $\alpha_{tot}/\alpha_{tot}^{0}$ and the $\Delta E_{gap}$ as represented in Figure 3a by full and empty symbols, respectively. The extent of $ArS^{-}$ ligand effect on the absorption spectrum of colloidal PbS QDs increases with increasing QD surface-to-volume ratio, therefore straightforwardly accounting for an effect exerted at the ligand/QD interface. Furthermore, such an effect is barely influenced by the dielectric constant of the surrounding solvent medium, as shown in Figure 3b.

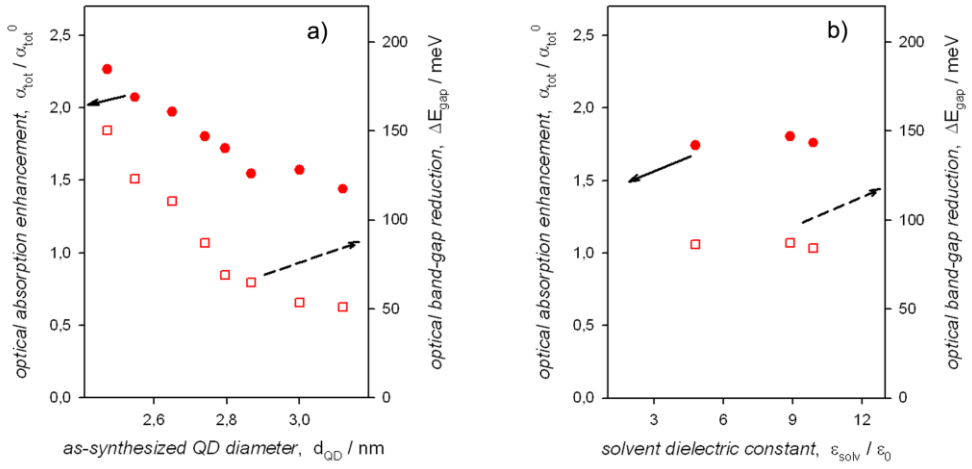


**Figure 3.** a) Plots of the broadband optical absorption enhancement ($\alpha_{tot}/\alpha_{tot}^{0}$, full circles) and of the optical band-gap reduction ($\Delta E_{gap}$, empty squares) upon complete oleate exchange with $ArS^{-}$ species at the surface of PbS QDs in dichloromethane solution as a function of as-synthesized QD diameter, $d_{QD}$. b) Plots of the broadband optical absorption enhancement ($\alpha_{tot}/\alpha_{tot}^{0}$, full circles) and of the optical band-gap reduction ($\Delta E_{gap}$, empty squares) upon complete oleate exchange with $ArS^{-}$ species at the surface of PbS QDs as a function of solvent dielectric constant, $\varepsilon_{solv}/\varepsilon_0$ (from left to right: chloroform, dichloromethane, and o-dichlorobenzene).

***The role of the ligands' pending moiety.*** In order to evaluate the replacing ligand effect on optical absorption properties of strongly quantum-confined PbS QDs with diameter of about 3 nm, we have thus systematically modified pending and anchoring moieties of the arenethiolate ligand framework (as shown in Scheme 1). Hence we have investigated whether the presence of electronically-active substituents in the para position of the benzenethiolate framework (see Scheme 1) may further affect optical absorption of colloidal PbS QDs. In presence of the electron-withdrawing trifluoromethyl group as for A-$ArS^-/Et_3NH^+$, the optical absorption increase (upon addition to PbS/Ol QDs in dichloromethane solution) is slightly lower than that induced by the addition of $ArS^-$ ligands, while a comparable bathochromic shift of the first excitonic peak is observed (Figure 4b and empty squares in Figure 4e-f); as for $ArS^-$ ligands, the spectral changes reach a plateau upon the addition of two A-$ArS^-$ ligands per $Pb_{exc}$, suggesting an analogously efficient coordination of PbS QD surface. Conversely, in presence of the electron-donor amino group as for D-$ArS^-/Et_3NH^+$, a much larger optical absorption enhancement can be achieved, whereas comparable $\Delta E_{gap}$ again accounts for a similar stoichiometry of the ligand exchanged species (Figure 4c and empty triangles in Figure 4e-f). Noticeably, the replacement of the conjugated moiety linked to the thiolate anchoring group with a saturated chain, as for AlSH, is accompanied by a slight absorption increase, while the $\Delta E_{gap}$ is analogous to that induced by aromatic thiolates (Figure 4d and full squares in Figure 4e-f). These findings clearly show that conjugated thiolate ligands drastically increase broadband optical absorption of colloidal PbS QDs which can be tuned and further enhanced by suitable electronically-active substituents; such an enhancement is observed in a broad spectral range (at energies below 3.5 eV), thus comprising the high energy region (above 3.1 eV, or below 400 nm) for which it has been previously found that (molar) absorption coefficient is not affected by quantum confinement.[6]

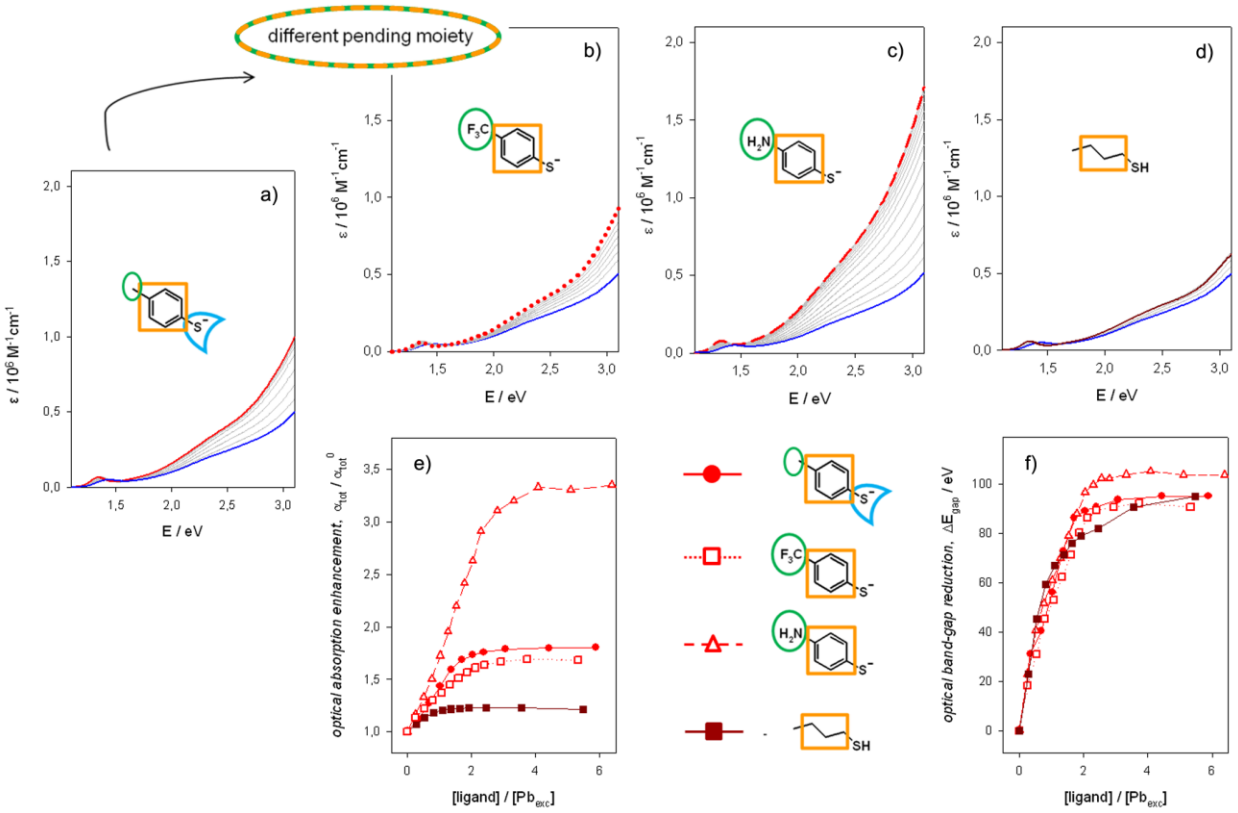


**Figure 4.** a-d) Optical absorption spectra of 2.5 μM dichloromethane solution of PbS/Ol QDs (blue spectra) upon addition of (a) $ArS^-/Et_3NH^+$, (b) A-$ArS^-/Et_3NH^+$, (c) D-$ArS^-/Et_3NH^+$, and (d) AlSH. Colored lines represent the spectra obtained at the plateau of the titration experiments. e-f) Plots of the corresponding broadband optical absorption enhancement ($\alpha_{tot}/\alpha_{tot}^0$, panel e) and of the optical band-gap reduction ($\Delta E_{gap}$, panel f) as a function of the number of replacing ligands added per excess Pb atoms on QD surface. Lines have been drawn to guide the eye only. Symbols representing each replacing ligand appear between $\alpha_{tot}/\alpha_{tot}^0$ and $\Delta E_{gap}$ plots.

In order to further investigate the origin of the observed ligand-induced spectral changes, we performed density functional (DFT) calculations with PBE functional[27] and def2-TZVP basis set[28] on model $(Pb_{55}S_{38})^{34+}$ clusters bearing 34 anionic species representing $Ol^-$, $ArS^-$, A-$ArS^-$, D-$ArS^-$, and $AlS^-$ ligands bound to external $Pb^{II}$ atoms (see Supporting Information for optimized structures). Such model systems aim at uncovering the role of the pending benzene ring (aliphatic chain) bearing electronically-active substituents on the density of states of our ligand/QD systems. The projected density of states (PDOS in Figure 5a-e) clearly show the relevant contribution of π orbitals localized on the ligands' aromatic portion to the density of states of the corresponding ligand/QD systems, together with the involvement of 3p orbitals of the S anchoring atom in the highest occupied ligand/QD states (whereas O anchoring atoms provide minor contribution). By time-dependent DFT calculations, performed with

same geometry, functional, and basis set as ground state ones, we calculated the optical absorption spectra displayed in Figure 5f, which show a drastic increase of the oscillator strength in presence of the benzene ring further enhanced by the amino group in para position, whereas absence of the conjugated pending moiety does not induce appreciable absorption enhancement, in agreement with experimental observations. Moreover, replacing ligands lead to a shift of the band energies of corresponding ligand/QD systems, in analogy to recent observation on PbS QD solids;[29] by introducing electronically-active substituents in para position of the benzenethiolate ligands, DFT calculations clearly show that withdrawing electrons from QD (with A-ArS$^-$ ligands, Figure 5c) lowers band energies, whereas pushing electron density towards the QD (with D-ArS$^-$ ligands, Figure 5d) raises band energies, thus suggesting the possibility to gain control on ionization potential and electron affinity of QDs via organic ligands.

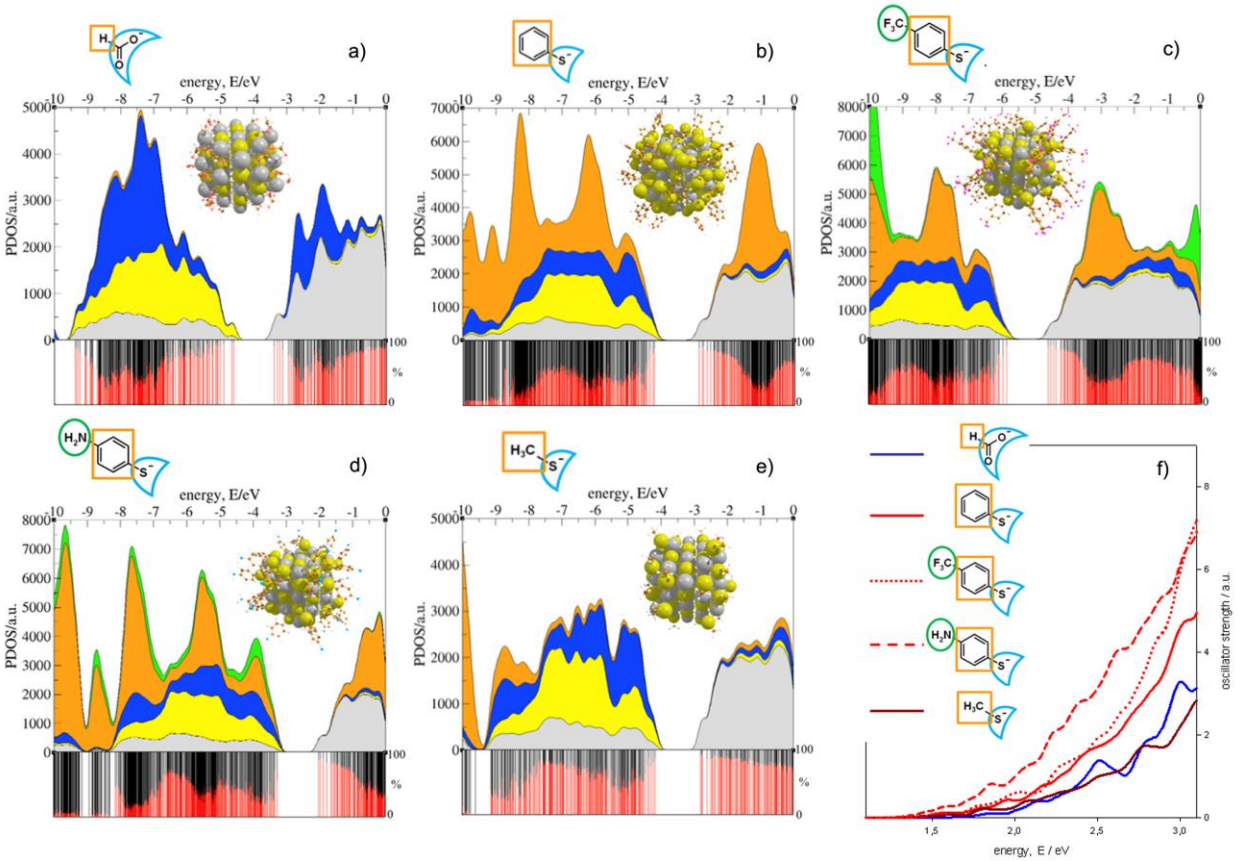


**Figure 5.** a-e) Projected density of states resulting from DFT calculations of the model $(Pb_{55}S_{38})^{34+}$ clusters capped with 34 anionic ligands, namely (a) $HCO_2^-$, (b) $C_6H_5S^-$, (c) $F_3C\text{-}C_6H_4S^-$, (d) $H_2N\text{-}C_6H_4S^-$, (e) $CH_3S^-$ which have been chosen in analogy to experimentally used ligands $OI^-$, $ArS^-$, $A\text{-}ArS^-$, $D\text{-}ArS^-$, AlSH, respectively. At the bottom of each PDOS plots appears the contribution of both ligands (in black) and inorganic cluster (in red) to the orbitals of the entire ligand/cluster system. Minimized ligand/QD model structures and ligands are shown in the corresponding PDOS panels. Cluster's Pb-localized orbitals are shown

in grey, cluster's S-localized orbitals in yellow, ligand's anchoring group-localized orbitals in blue, orbitals localized on the backbone of ligand's pending group in orange, and orbitals localized on the sustituents of ligand's pending group in green, according to colors used to represent ligand/cluster structures. f) Corresponding time-dependent DFT calculated absorption spectra; legend appears on the left side of the panel.

Ground state DFT calculations are qualitatively consistent with the experimental findings, thus accounting for strong ligand/QD electronic interactions. Conversely, the absorption onset of the employed thiolate ligands (≥ 3.5 eV) excludes that the enhancement of solar-light absorption could be trivially attributed to their contribution, whereas polarization effect (or solvatochromism) is expected to barely affect optical absorption spectra, as shown by changing the dielectric constant of the surrounding medium (Figure 2b); moreover, by using a two-level nearly free electron model[30] to describe the first excitonic transition of our inorganic core/ ligand shell/ solvent medium system (see Supporting Information for details), the polarization effect induced by the replacing ligand shell negligibly affects both the local electric field[31,32] and the energy of the optical band-gap.[33,34] Indeed, DFT calculations suggest that orbitals localized on the conjugated thiolate ligands largely contribute to the density of states of the ligand/QD system. This is corroborated by calculating the contribution of organic and inorganic components to the entire ligand/cluster orbitals which shows that orbital mixing is involved in essentially every electronic state of the ligand/QD system (see at the bottom of panels a-e in Figure 5). Therefore, coupling of QD localized orbitals with partially mixed π orbitals of the benzene ring and non-bonding orbitals localized on the S anchoring atom[35] leads to broadly increase the density of states thus inducing the observed optical absorption enhancement, whereas contribution from 3p orbitals localized on the sulfur anchoring atom to the density of the highest occupied states is likely responsible for the optical band-gap reduction.

***The role of ligands' anchoring group.*** We have thus modified the binding moiety on the p-methylbenzene group of the replacing ligands in order to elucidate the role exerted by the chemical nature and bonding mode of the anchoring groups on the optical absorption properties of colloidal PbS QDs. To this aim, we have synthesized p-methylbenzenedithoate ligands as triethylammonium salt ($ArCS_2^-/Et_3NH^+$). Upon addition of such bi-dentate S-terminated ligand to PbS/Ol QDs solution in the same experimental conditions as previously discussed for mono-dentate thiolate ligands, we observe a much higher absorbance increase for the same number of added replacing ligands (Figure 6a and empty circles in Figure 6b), although resulting QDs show poorer colloidal stability. We

notice that $ArCS_2^-$ addition induces a smaller bathochromic shift of the first excitonic peak compared to $ArS^-$ ligands and that the plot of $\Delta E_{gap}$ reaches a plateau for only one $ArCS_2^-$ ligand per $Pb_{exc}$ (empty circles in Figure 6c); in this regard, is worth mentioning that previous reports on PbS/Ol QDs obtained with similar synthetic procedure have demonstrated the presence of one oleate ligand per $Pb_{exc}$, while charges are balanced by $OH^-$ anions produced during lead(II)-oleate homoleptic complexes formation.[36] The saturation effect observed for one $ArCS_2^-$ ligand per $Pb_{exc}$ and the concomitant poor colloidal stability of the resulting species may result from the large strain induced on PbS QDs induced by $ArCS_2^-$ ligands as suggested by DFT calculation (structure of corresponding cluster $Pb_{55}S_{38}(C_6H_5CS_2)_{34}$ is shown on top of Figure 6a and Supporting Figure S11). Furthermore, addition of bi-dentate O-terminated ligands $ArCO_2^-/Et_3NH^+$ leads to slight spectral changes (which again reach a plateau for one $ArCO_2^-$ ligand per $Pb_{exc}$, full triangles in Figure 6b-c), whereas addition of N-terminated ligands, $ArNH_2$, does not induce appreciable spectral changes (full squares in Figure 6b-c) which can be ascribed to poor QD surface coordination; neutral $ArNH_2$ ligands are expected to replace $Pb^{II}(Ol^-)_2$ complexes from QD surface and the lack of hypsochromic shift observed accounts for weak coordination to PbS QD surface, whereas $ArCO_2^-$ ligands may partially displace pristine oleate ligands since aromatic carboxylates are weaker and more polarizable bases than aliphatic carboxylates. Conversely, the soft character of S-terminated bases leads to more stable coordination interactions with $Pb^{II}$ cations, thus implying that the amino group of D-$ArS^-$ ligand does not appreciably contribute to or alter the coordination to QD surface, which is therefore expected to occur exclusively via the thiolate moiety.

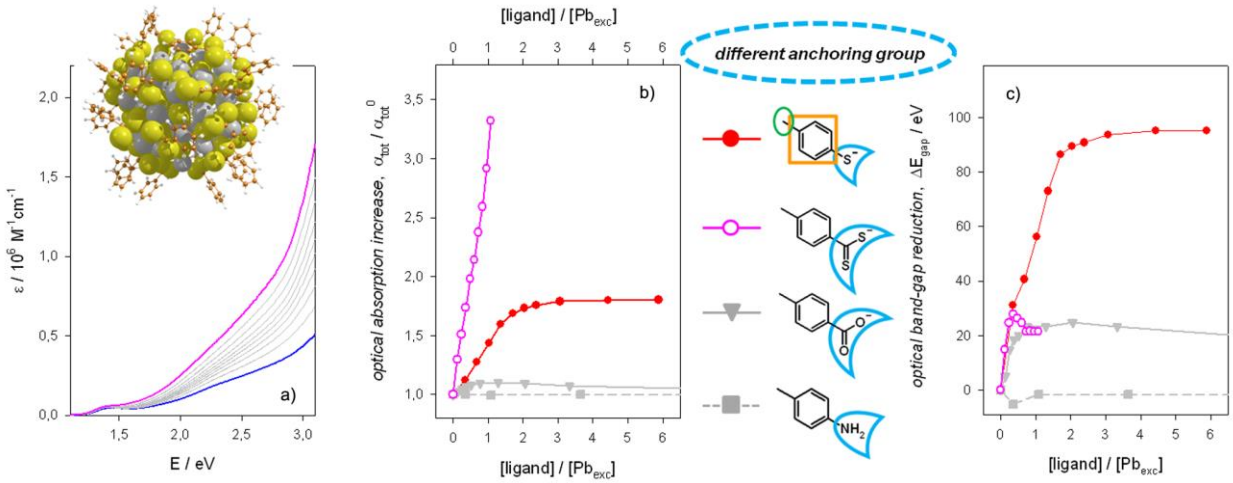


**Figure 6.** a) Optical absorption spectra of 2.5 µM dichloromethane solution of PbS/Ol QDs (blue spectrum) upon addition of $ArCS_2^-/Et_3NH^+$. Purple line represents the spectrum obtained at the end of the titration experiments. Optimized structure of the

calculated $Pb_{55}S_{38}(C_6H_5CS_2)_{34}$ is shown, highlighting inorganic cluster distortion upon ligand binding. b-c) Plots of the corresponding broadband optical absorption enhancement ($\alpha_{tot}/\alpha_{tot}^0$, panel b) and of the optical band-gap reduction ($\Delta E_{gap}$, panel c) as a function of the number of replacing ligands added per excess Pb atoms on QD surface. Lines have been drawn to guide the eye only. Symbols representing replacing ligands are drawn between $\alpha_{tot}/\alpha_{tot}^0$ and $\Delta E_{gap}$ plots.

***On the absorption coefficient of colloidal PbS QDs at high energies.*** The systematic investigation of the ligand effect on the optical absorption properties of colloidal PbS QDs clearly shows that S-terminated ligands bearing a conjugated moiety induce a large absorbance increase, which is particularly relevant at high energies (above 3.1 eV, or below 400 nm) where it has been previously reported that molar absorption coefficient ($\varepsilon_{400nm}$) is not affected by quantum confinement.[6,31] Indeed, we measure $\varepsilon_{400nm}$ values which are up to 340 % larger than those previously reported for colloidal PbS QDs (see Table 1). Such $\varepsilon_{400nm}$ values are larger for bi-dentate conjugated dithioate ligands ($ArCS_2^-$) compared to mono-dentate conjugated thiolates ($ArS^-$) for the same number of added replacing ligands, whereas slight $\varepsilon_{400nm}$ increase is induced by saturated thiols (AlSH). This observation points out the significance of the $\pi$ character of the entire replacing ligand on the QD optical absorption properties, which can be tuned and further enhanced via electron-donating substituents (as for D-$ArS^-$) increasing the electron density of the organic shell.

**Table 1.** Values of molar absorption coefficient at 400 nm ($\varepsilon_{400nm}$), broadband optical absorption increase ($\alpha_{tot}/\alpha_{tot}^0$), and optical bandgap reduction ($\Delta E_{gap}$) obtained for colloidal PbS QDs in presence of 400 equivalents of the ligands (at the plateau of the titration experiments) indicated in the left column and shown in the library of Scheme 1. All values have been determined upon spectrophotometric titrations of as-synthesized PbS/Ol QDs in dichloromethane solution with the replacing ligands' solutions in a quartz cuvette and under the assumption that $\varepsilon_{400nm}$ = 510000 $M^{-1}cm^{-1}$ for PbS/Ol QDs with a diameter of 2.8 nm.[6]

| Colloidal PbS QDs capped with: | $\varepsilon_{400nm}$ / $10^6$ $M^{-1}cm^{-1}$ | $\alpha_{tot}/\alpha_{tot}^0$ | $\Delta E_{gap}$ / meV |
|---|---|---|---|
| **$ArS^-$** | **1.0** | **1.8** | **92** |
| **A-$ArS^-$** | **0.93** | **1.7** | **90** |
| **D-$ArS^-$** | **1.7** | **3.3** | **100** |
| **$AlS^-$** | **0.64** | **1.2** | **92** |
| **$ArCS_2^-$** [a] | **1.7 (1.3[b])** | **3.3 (2.9[b])** | **22** |
| **$ArCO_2^-$** | **0.58** | **1.1** | **24** |
| **$ArNH_2$** | **0.51** | **1.0** | **0.0** |

[a]Values obtained upon addition of 150 equivalents of $ArCS_2^-/Et_3NH^+$ ligands due to the poor colloidal stability of the resulting system. [b]Values in parentheses were obtained upon subtracting the contribution of $ArCS_2^-/Et_3NH^+$ ligand to the absorption spectrum.

According to DFT calculations (see above), the conjugated S-terminated ligands coordinated to the PbS QD surface both increase the density of states and the oscillator strength of the resulting ligand/QD system via electronic coupling of the organic and inorganic components. Such an electronic coupling gives rise to peculiar chemical species displaying properties that cannot be described as the mere sum of those of the ligand and QD components: indeed, this clearly emerges comparing the calculated orbitals for the entire ligand/cluster system (denoted as $Pb_{55}S_{38}(ligand)_{34}$ in Figure 7, where ligand is (a) $HCO_2$, (b) $C_6H_5S$, (c) $F_3C$-$C_6H_4S$, (d) $H_2N$-$C_6H_4S$, (e) $CH_3S$) with the orbitals of ligands and cluster experiencing each other electric field (referred to as $(Pb_{55}S_{38})^{34+}\cdot[34(ligand^-)]$ in Figure 7) and by analyzing ratiometric and differential absorption spectra shown in Figure S15. The QD surface-to-volume ratio dependence of the observed optical absorption increase (empty circles in Figure 2a) accounts for an interfacial ligand/QD effect, which becomes extremely large in the strong quantum confinement regime experienced by small QDs[37] and therefore these two effects cannot be straightforwardly disentangled.

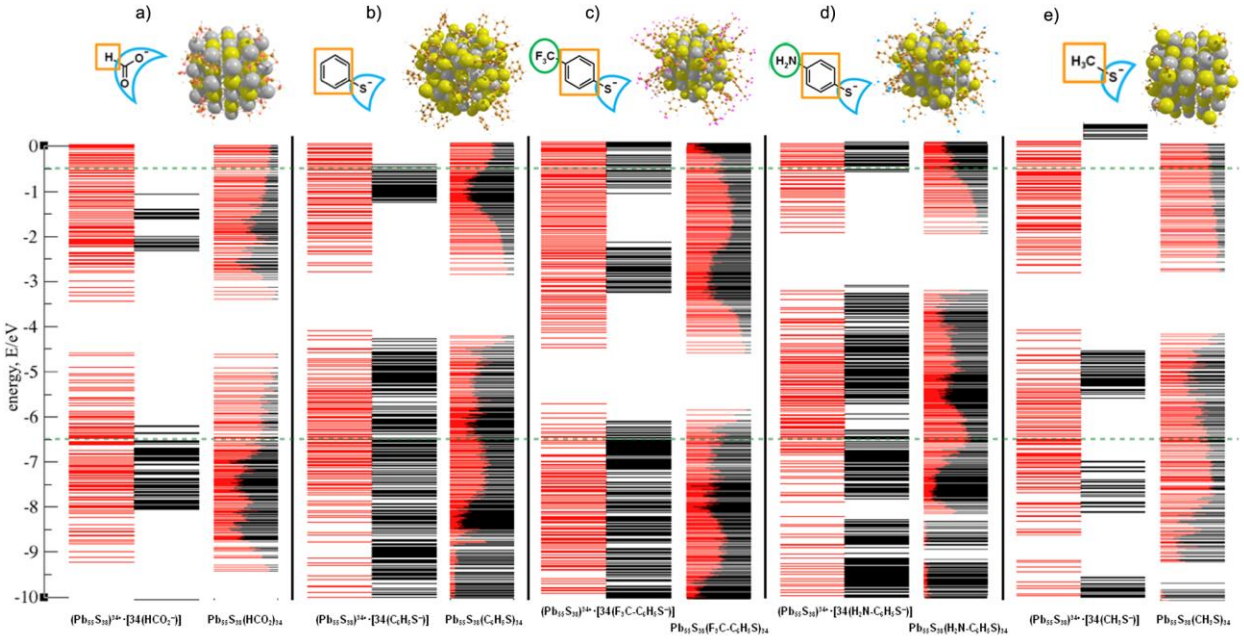


**Figure 7.** Calculated ligand/cluster orbitals for the model $(Pb_{55}S_{38})^{34+}$ clusters capped with 34 anionic ligands, namely (a) $HCO_2^-$, (b) $C_6H_5S^-$, (c) $F_3C$-$C_6H_4S^-$, (d) $H_2N$-$C_6H_4S^-$, (e) $CH_3S^-$ which have been chosen in analogy to experimentally used ligands $Ol^-$, $ArS^-$, A-$ArS^-$, D-$ArS^-$, AlSH, respectively, showing the contribution of organic ligands (in black) and inorganic core (in red). Orbitals appearing on the right side of each panel are those of the entire ligand/cluster system (denoted as $Pb_{55}S_{38}(ligand)_{34}$, where ligand stands for (a) $HCO_2$, (b) $C_6H_5S$, (c) $F_3C$-$C_6H_4S$, (d) $H_2N$-$C_6H_4S$, (e) $CH_3S$), whereas orbitals on the left side represent contribution of ligands and core in each other electric field (referred to as $(Pb_{55}S_{38})^{34+}\cdot[34(ligand^-)]$). Dotted green lines

limit the range of orbitals contributing to the calculated optical absorption shown in Figure 4f below 3.1 eV. Minimized ligand/QD model structures and ligands are shown in the corresponding orbitals' panels.

***On the origin of the excitonic red-shift commonly observed for thiol-treated PbS QD solids.*** Thiolate-terminated ligands also induce a noticeable optical band gap reduction regardless of the nature of the appended moieties (aromatic or aliphatic). This again reflects the impact of 3p orbitals localized on S anchoring atom which contribute to higher occupied states of the resulting ligand/QD systems and can therefore account for the origin of the bathochromic shift commonly observed after the post-deposition treatment of lead-chalcogenide QD solids with short thiol-terminated molecules.[38] Indeed, the addition of thiolate-terminated ligands to PbS/Ol QDs with diameter of 2.8 nm induces a bathochromic shift of the first excitonic peak of about 90 meV (slightly dependent on the nature of the pending groups, as shown in Figure 4f), whereas solids obtained from purified PbS/ArS QDs are characterized by an extra red-shift of about 10 meV (Figure 8). Our ligand exchange approach guarantees the successful attainment of colloidal thiolate-capped PbS QDs that are free-standing in solution-phase, and then self-assemblies thereof, allowing us to discriminate between intra- and inter-QD interactions, whereas solid-phase ligand exchange hinders such a distinction. On this basis, the observed optical band gap reduction in solids may be prevalently (~ 90 %) ascribed to the contribution of interfacial interactions between the (S)3p orbitals of the thiolate-terminated ligands and the (Pb)6p core orbitals. The extra red-shift observed in solid-phase can be instead attributed to inter-QD excitonic (dipole-dipole) coupling, whereas inter-QD electronic coupling is negligible due the low field-effect mobility observed in PbS/ArS QD solids,[13] according to the Einstein-Smoluchowski relation. Other mechanisms already envisaged to explain the ligand-induced red-shift of the first excitonic peak in PbS QD solids are not applicable to our system. For instance, exciton delocalization on the ligand shell attributable to the resonance between the highest occupied states of the QDs and the ligands,[15] is only partially appropriate to our systems since employed ligands have frontier molecular orbitals[39] which differs in energy by several electronvolts, thus resonance with QD valence and conduction band edges[40] would be expected to be largely different while we observe analogous red shift (see Figure 4f). Further explanation based on quantum-confined Stark effect[41] is unlikely since the ligand-induced red-shift would be expected to increase for larger QDs,[42] while we observe the opposite dependence (Figure 2a). Furthermore, our results point out that previously proposed replacing ligand-induced polarization effect, or solvatochromism,[43] can be considered negligible as demonstrated by poor spectral dependence on dielectric constant

of the solvent (Figure 2b) and by calculations based on effective medium approximation (see Supporting Information).

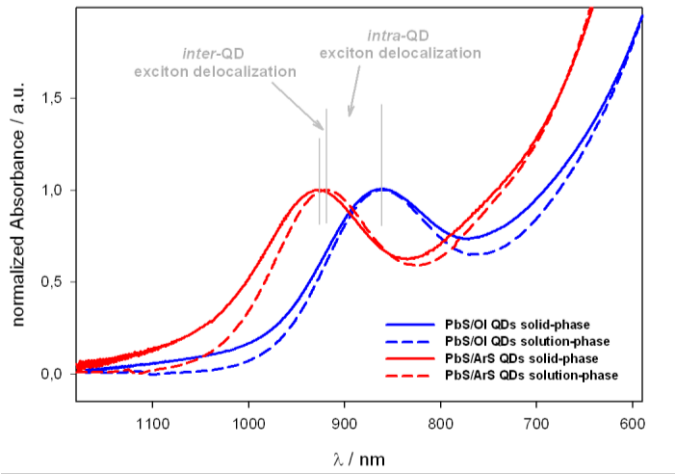


**Figure 8.** Optical absorption spectra of solution-phase (dashed lines) and solid-phase (solid lines) PbS/Ol QDs (blue lines) and PbS/ArS QDs (red lines) normalized at the maximum of the first excitonic peak. Vertical grey lines have been drawn to emphasize the bathochromic shift of the first excitonic peak occurring upon solution-phase ligand exchange of PbS/Ol QDs to PbS/ArS QDs and then to solids therof.

**Conclusion.**

In this study we have described a novel design concept for light-harvesting nanomaterials to be applied in solution-processed photovoltaic and photodetection applications. Indeed, we have demonstrated that suitable QD surface modification with short conjugated organic molecules permits to enhance (> 300 %) broadband light absorption of PbS QDs, while preserving good long-term colloidal stability. Such a design concept is based on the evidence that organic ligands and inorganic cores constituting the colloidal semiconductor nanocrystals are inherently electronically coupled materials, therefore rational design of the organic shell gives rise to ligand/QD species displaying enhanced optical absorption properties that could not be predicted or even conceived on the basis of ligand and QD components. Here we have provided systematic investigation of ground-state ligand/QD interactions leading to such a drastic enhancement of broadband optical absorption and described the prominent role exerted by the chemical nature and coordination geometry of the anchoring group and its π conjugation with the pending moiety which mediate the electronic coupling with the PbS QD cores. Noteworthly, similar optical absorption changes are observed upon addition of $ArS^{-}/Et_3NH^{+}$ to oleate-capped CdS QDs[44] (see Supporting Figure S16), thus

suggesting possible general applicability of the principles here presented and described. Conversely, the absorption spectra of colloidal CdS and CdSe/CdS core/(elongated)shell QDs capped with aliphatic phosphine oxide and phosphonic acid ligands[45] are slightly affected by arenethiolate ligands (see Supporting Figure S16). As already discussed, carboxylates rather weakly coordinate large, highly polarizable $Pb^{II}$ and $Cd^{II}$ cations and therefore are easily replaced by thiolate-terminated ligands, whereas phosphine oxide- and phoshonic acid-based ligands, commonly considered as soft bases are expected to stably bind Cd atoms at the QD surface and therefore are less easily replaced by thiolates. These findings result in a simple and effective approach to enhance and tune broadband solar-light absorption of colloidal metal-chalcogenide QDs, which could be exploited for the design of light-harvesting systems to be applied for solution-processed photovoltaic and photodetection applications; the employed short ligands reduce inter-QD distance in solids[13,14] and may eventually further increase optical absorption via dipolar coupling,[46] representing a relevant contribution to the optimization of photo-active QD layer thickness which ultimately mediates absorption of the incident light and transport of photo-generated charges thus affecting photon-to-charge carrier conversion efficiencies.

**SUPPORTING INFORMATION AVAILABLE.**

Details on the synthesis of colloidal QDs; spectroscopic characterization of replacing ligands; TEM images of QDs; details on DFT and effective medium approximation calculations are available free of charge via the Internet at http://pubs.acs.org.

**CORRESPONDING AUTHOR.**

*e-mail: carlo.giansante@iit.it

**ACKNOWLEDGEMENTS.**

We thank Luigi Carbone and Giovanni Lerario for fruitful discussion. This work was supported by Progetto di ricerca PON R&C 2007-2013 (Avviso n. 713/Ric. del 29 ottobre 2010) MAAT-Molecular NAnotechnology for HeAlth and EnvironmenT (Project Number: PON02_00563_3316357), EFOR-Energia da FOnti Rinnovabili (Iniziativa CNR per il Mezzogiorno L. 191/2009 art. 2 comma 44), and by the European project ESCORT- Efficient Solar Cells based on Organic and hybrid Technology (7th FWP - reference number 261920).

**REFERENCES.**


1. Kim, J. Y.; Voznyy, O.; Zhitomirsky, D.; Sargent, E. H., 25th Anniversary Article: Colloidal Quantum Dot Materials and Devices: A Quarter-Century of Advances. *Advanced Materials* **2013,** *25* (36), 4986-5010.

2. Yin, Y.; Alivisatos, A. P., Colloidal nanocrystal synthesis and the organic-inorganic interface. *Nature* **2005,** *437* (7059), 664-670.

3. Talapin, D. V.; Lee, J.-S.; Kovalenko, M. V.; Shevchenko, E. V., Prospects of Colloidal Nanocrystals for Electronic and Optoelectronic Applications. *Chemical Reviews* **2009,** *110* (1), 389-458.

4. Peterson, M. D.; Cass, L. C.; Harris, R. D.; Edme, K.; Sung, K.; Weiss, E. A., The Role of Ligands in Determining the Exciton Relaxation Dynamics in Semiconductor Quantum Dots. *Annual Review of Physical Chemistry* **2014,** *65* (1), 317-339.

5. Fischer, S. A.; Crotty, A. M.; Kilina, S. V.; Ivanov, S. A.; Tretiak, S., Passivating ligand and solvent contributions to the electronic properties of semiconductor nanocrystals. *Nanoscale* **2012,** *4* (3), 904-914.

6. Moreels, I.; Lambert, K.; Smeets, D.; De Muynck, D.; Nollet, T.; Martins, J. C.; Vanhaecke, F.; Vantomme, A.; Delerue, C.; Allan, G.; Hens, Z., Size-Dependent Optical Properties of Colloidal PbS Quantum Dots. *ACS Nano* **2009,** *3* (10), 3023-3030.

7. Konstantatos, G.; Howard, I.; Fischer, A.; Hoogland, S.; Clifford, J.; Klem, E.; Levina, L.; Sargent, E. H., Ultrasensitive solution-cast quantum dot photodetectors. *Nature* **2006,** *442* (7099), 180-183.

8. Hinds, S.; Levina, L.; Klem, E. J. D.; Konstantatos, G.; Sukhovatkin, V.; Sargent, E. H., Smooth-Morphology Ultrasensitive Solution-Processed Photodetectors. *Advanced Materials* **2008,** *20* (23), 4398-4402.

9. Law, M.; Luther, J. M.; Song, Q.; Hughes, B. K.; Perkins, C. L.; Nozik, A. J., Structural, Optical, and Electrical Properties of PbSe Nanocrystal Solids Treated Thermally or with Simple Amines. *Journal of the American Chemical Society* **2008,** *130* (18), 5974-5985.

10. Gao, Y.; Aerts, M.; Sandeep, C. S. S.; Talgorn, E.; Savenije, T. J.; Kinge, S.; Siebbeles, L. D. A.; Houtepen, A. J., Photoconductivity of PbSe Quantum-Dot Solids: Dependence on Ligand Anchor Group and Length. *ACS Nano* **2012,** *6* (11), 9606-9614.

11. Dong, A.; Ye, X.; Chen, J.; Kang, Y.; Gordon, T.; Kikkawa, J. M.; Murray, C. B., A Generalized Ligand-Exchange Strategy Enabling Sequential Surface Functionalization of Colloidal Nanocrystals. *Journal of the American Chemical Society* **2010,** *133* (4), 998-1006.

12. Fafarman, A. T.; Koh, W.-k.; Diroll, B. T.; Kim, D. K.; Ko, D.-K.; Oh, S. J.; Ye, X.; Doan-Nguyen, V.; Crump, M. R.; Reifsnyder, D. C.; Murray, C. B.; Kagan, C. R., Thiocyanate-Capped Nanocrystal Colloids: Vibrational Reporter of Surface Chemistry and Solution-Based Route to Enhanced Coupling in Nanocrystal Solids. *Journal of the American Chemical Society* **2011,** *133* (39), 15753-15761.

13. Giansante, C.; Carbone, L.; Giannini, C.; Altamura, D.; Ameer, Z.; Maruccio, G.; Loiudice, A.; Belviso, M. R.; Cozzoli, P. D.; Rizzo, A.; Gigli, G., Colloidal Arenethiolate-Capped PbS Quantum Dots: Optoelectronic Properties, Self-Assembly, and Application in Solution-Cast Photovoltaics. *The Journal of Physical Chemistry C* **2013,** *117* (25), 13305-13317.

14. Giansante, C.; Carbone, L.; Giannini, C.; Altamura, D.; Ameer, Z.; Maruccio, G.; Loiudice, A.; Belviso, M. R.; Cozzoli, P. D.; Rizzo, A.; Gigli, G., Surface chemistry of arenethiolate-capped PbS quantum dots and application as colloidally stable photovoltaic ink. *Thin Solid Films* **2014,** *560* (0), 2-9.

15. Frederick, M. T.; Amin, V. A.; Cass, L. C.; Weiss, E. A., A Molecule to Detect and Perturb the Confinement of Charge Carriers in Quantum Dots. *Nano Letters* **2011,** *11* (12), 5455-5460.

16. Fischer, A.; Rollny, L.; Pan, J.; Carey, G. H.; Thon, S. M.; Hoogland, S.; Voznyy, O.; Zhitomirsky, D.; Kim, J. Y.; Bakr, O. M.; Sargent, E. H., Directly Deposited Quantum Dot Solids Using a Colloidally Stable Nanoparticle Ink. *Advanced Materials* **2013,** *25* (40), 5742-5749.

17. Danehy, J. P.; Parameswaran, K. N., Acidic dissociation constants of thiols. *Journal of Chemical & Engineering Data* **1968,** *13* (3), 386-389.

18. Masui, M.; Sayo, H.; Tsuda, Y., Anodic oxidation of amines. Part I. Cyclic voltammetry of aliphatic amines at a stationary glassy-carbon electrode. *Journal of the Chemical Society B: Physical Organic* **1968,** (0), 973-976.

19. Hines, M. A.; Scholes, G. D., Colloidal PbS Nanocrystals with Size-Tunable Near-Infrared Emission: Observation of Post-Synthesis Self-Narrowing of the Particle Size Distribution. *Advanced Materials* **2003,** *15* (21), 1844-1849.

20. Anderson, N. C.; Hendricks, M. P.; Choi, J. J.; Owen, J. S., Ligand Exchange and the Stoichiometry of Metal Chalcogenide Nanocrystals: Spectroscopic Observation of Facile Metal-Carboxylate Displacement and Binding. *Journal of the American Chemical Society* **2013,** *135* (49), 18536-18548.

21. Gomes, R.; Hassinen, A.; Szczygiel, A.; Zhao, Q.; Vantomme, A.; Martins, J. C.; Hens, Z., Binding of Phosphonic Acids to CdSe Quantum Dots: A Solution NMR Study. *The Journal of Physical Chemistry Letters* **2011,** *2* (3), 145-152.

22. Cademartiri, L.; Montanari, E.; Calestani, G.; Migliori, A.; Guagliardi, A.; Ozin, G. A., Size-Dependent Extinction Coefficients of PbS Quantum Dots. *Journal of the American Chemical Society* **2006,** *128* (31), 10337-10346.

23. Moreels, I.; Fritzinger, B.; Martins, J. C.; Hens, Z., Surface Chemistry of Colloidal PbSe Nanocrystals. *Journal of the American Chemical Society* **2008,** *130* (45), 15081-15086.

24. Hughes, B. K.; Ruddy, D. A.; Blackburn, J. L.; Smith, D. K.; Bergren, M. R.; Nozik, A. J.; Johnson, J. C.; Beard, M. C., Control of PbSe Quantum Dot Surface Chemistry and Photophysics Using an Alkylselenide Ligand. *ACS Nano* **2012,** *6* (6), 5498-5506.

25. Jasieniak, J.; Mulvaney, P., From Cd-Rich to Se-Rich − the Manipulation of CdSe Nanocrystal Surface Stoichiometry. *Journal of the American Chemical Society* **2007,** *129* (10), 2841-2848.

26. Shaw, R. A.; Woods, M., Preparation and some properties of lead thiolates. *Journal of the Chemical Society A: Inorganic, Physical, Theoretical* **1971,** (0), 1569-1571.

27. Adamo, C.; Barone, V., Toward reliable density functional methods without adjustable parameters: The PBE0 model. *The Journal of Chemical Physics* **1999,** *110* (13), 6158-6170.

28. Weigend, F.; Furche, F.; Ahlrichs, R., Gaussian basis sets of quadruple zeta valence quality for atoms H–Kr. *The Journal of Chemical Physics* **2003,** *119* (24), 12753-12762.

29. Brown, P. R.; Kim, D.; Lunt, R. R.; Zhao, N.; Bawendi, M. G.; Grossman, J. C.; Bulović, V., Energy Level Modification in Lead Sulfide Quantum Dot Thin Films through Ligand Exchange. *ACS Nano* **2014,** *8* (6), 5863-5872.

30. Brus, L. E., Electron–electron and electron-hole interactions in small semiconductor crystallites: The size dependence of the lowest excited electronic state. *The Journal of Chemical Physics* **1984,** *80* (9), 4403-4409.

31. Hens, Z.; Moreels, I., Light absorption by colloidal semiconductor quantum dots. *Journal of Materials Chemistry* **2012,** *22* (21), 10406-10415.

32. Neeves, A. E.; Birnboim, M. H., Composite structures for the enhancement of nonlinear-optical susceptibility. *J. Opt. Soc. Am. B* **1989,** *6* (4), 787-796.

33. Leatherdale, C. A.; Bawendi, M. G., Observation of solvatochromism in CdSe colloidal quantum dots. *Physical Review B* **2001,** *63* (16), 165315.

34. Allan, G.; Delerue, C.; Lannoo, M.; Martin, E., Hydrogenic impurity levels, dielectric constant, and Coulomb charging effects in silicon crystallites. *Physical Review B* **1995,** *52* (16), 11982-11988.

35. Aoki, M.; Kamada, T.; Sasaki, K.; Masuda, S.; Morikawa, Y., Chemisorption-induced gap states at organic-metal interfaces: benzenethiol and benzeneselenol on metal surfaces. *Physical Chemistry Chemical Physics* **2012,** *14* (12), 4101-4108.

36. Zherebetskyy, D.; Scheele, M.; Zhang, Y.; Bronstein, N.; Thompson, C.; Britt, D.; Salmeron, M.; Alivisatos, P.; Wang, L.-W., Hydroxylation of the surface of PbS nanocrystals passivated with oleic acid. *Science* **2014,** *344* (6190), 1380-1384.

37. Wise, F. W., Lead Salt Quantum Dots: the Limit of Strong Quantum Confinement. *Accounts of Chemical Research* **2000,** *33* (11), 773-780.

38. Choi, J. J.; Luria, J.; Hyun, B.-R.; Bartnik, A. C.; Sun, L.; Lim, Y.-F.; Marohn, J. A.; Wise, F. W.; Hanrath, T., Photogenerated Exciton Dissociation in Highly Coupled Lead Salt Nanocrystal Assemblies. *Nano Letters* **2010,** *10* (5), 1805-1811.

39. Oliver, T. A. A.; Zhang, Y.; Ashfold, M. N. R.; Bradforth, S. E., Linking photochemistry in the gas and solution phase: S-H bond fission in p-methylthiophenol following UV photoexcitation. *Faraday Discussions* **2011,** *150* (0), 439-458.

40. Jasieniak, J.; Califano, M.; Watkins, S. E., Size-Dependent Valence and Conduction Band-Edge Energies of Semiconductor Nanocrystals. *ACS Nano* **2011,** *5* (7), 5888-5902.

41. Yaacobi-Gross, N.; Soreni-Harari, M.; Zimin, M.; Kababya, S.; Schmidt, A.; Tessler, N., Molecular control of quantum-dot internal electric field and its application to CdSe-based solar cells. *Nat Mater* **2011,** *10* (12), 974-979.

42. Wen, G. W.; Lin, J. Y.; Jiang, H. X.; Chen, Z., Quantum-confined Stark effects in semiconductor quantum dots. *Physical Review B* **1995,** *52* (8), 5913-5922.

43. Wolcott, A.; Doyeux, V.; Nelson, C. A.; Gearba, R.; Lei, K. W.; Yager, K. G.; Dolocan, A. D.; Williams, K.; Nguyen, D.; Zhu, X. Y., Anomalously Large Polarization Effect Responsible for Excitonic Red Shifts in PbSe Quantum Dot Solids. *The Journal of Physical Chemistry Letters* **2011,** *2* (7), 795-800.

44. Yu, W. W.; Peng, X., Formation of High-Quality CdS and Other II–VI Semiconductor Nanocrystals in Noncoordinating Solvents: Tunable Reactivity of Monomers. *Angewandte Chemie International Edition* **2002,** *41* (13), 2368-2371.

45. Carbone, L.; Nobile, C.; De Giorgi, M.; Sala, F. D.; Morello, G.; Pompa, P.; Hytch, M.; Snoeck, E.; Fiore, A.; Franchini, I. R.; Nadasan, M.; Silvestre, A. F.; Chiodo, L.; Kudera, S.; Cingolani, R.; Krahne, R.; Manna, L., Synthesis and Micrometer-Scale Assembly of Colloidal CdSe/CdS Nanorods Prepared by a Seeded Growth Approach. *Nano Letters* **2007,** *7* (10), 2942-2950.

46. Geiregat, P.; Justo, Y.; Abe, S.; Flamee, S.; Hens, Z., Giant and Broad-Band Absorption Enhancement in Colloidal Quantum Dot Monolayers through Dipolar Coupling. *ACS Nano* **2013,** *7* (2), 987-993.